Hindawi
Advances in Materials Science and Engineering
Volume 2022, Article ID 6705354, 18 pages
https://doi.org/10.1155/2022/6705354

Research Article

Experimental Study on the Performance of Basalt Fiber Modified Pervious Concrete Based on Entropy Method

Wenhua Wang,[1] Xiaojun Cheng,[2] Jinzhong Zhu,[2] Da Jiang,[2] Hongliang Sun,[3] and Siyu Liu[4]

[1]*School of Civil Engineering of Changchun Institute of Technology, Jilin Province Key Laboratory for Earthquake Resistance and Hazard Mitigation of Civil Engineering, Changchun, Jilin 130012, China*
[2]*School of Civil Engineering of Changchun Institute of Technology, Changchun, Jilin 130012, China*
[3]*Changchun Municipal Engineering & Research Institute Co Ltd, Changchun, Jilin 130012, China*
[4]*Ccccshec Fourth Engineering Company Ltd, Wuhu, Anhui 241000, China*

Correspondence should be addressed to Xiaojun Cheng; chengxiaojun@stu.ccit.edu.cn

Received 30 July 2022; Revised 9 November 2022; Accepted 15 November 2022; Published 28 November 2022

Academic Editor: Laurent Lebrun

In order to solve the problem the permeability coefficient and strength of pervious concrete pavement are difficult to coordinate. In this paper, the basalt fiber was incorporated into pervious concrete, and the single factor control variable method was used to carry out the test of basalt fiber modified pervious concrete, and combined with the microstructure image, the influence law of different diameters, lengths, and dosages of basalt fibers on mechanical properties and pervious properties of pervious concrete were studied. The optimal incorporation index of basalt fiber was determined by a new analysis method—the entropy method. Finally, it is concluded that basalt fiber can improve the mechanical and pervious properties of pervious concrete by changing the internal structure of pervious concrete. In addition, when the diameter of basalt fiber increases from 14 μm to 20 μm, the compressive strength of pervious concrete decreases by 17.79%. The splitting tensile strength showed a trend of increasing to decreasing. The porosity and water permeability increased by 2.55% and 48.66%, respectively. When the basalt fiber length increases from 12 mm to 24 mm, the compressive strength of pervious concrete increases by 20.54%, and the splitting tensile strength increases first and then decreases. The porosity and water permeability increased by 6.40% and 57.68%, respectively. When the content of basalt fiber increases from 2 kg/m^3 to 6 kg/m^3, the compressive strength of pervious concrete decreases by 16.25%. The splitting tensile strength increases by 23.72%. The porosity and permeability decreased by 7.75% and 39.36%, respectively. Finally, the entropy method is used to comprehensively analyze the optimum incorporation indexes of basalt fiber, which can achieve the optimal mechanical properties and water permeability at the same time with, 20 μm in diameter, 24 mm in length, and 2 kg/m^3 in dosage, and it provides a reference value for the popularization and application of basalt fiber pervious concrete in practical engineering.

1. Introduction

As an eco-environmental protection road surface, pervious concrete pavement is an important infrastructure for sponge city construction [1–3]. In recent years, pervious concrete has been more and more used in landscape roads, park squares, urban tree pools, recreational paths, and other pervious pavement fields. However, it is found in practical engineering that the strength of pervious concrete is much lower than that of ordinary concrete because the external force borne and transmitted by pervious concrete are mainly completed by the contact points between aggregates, and the strength of pervious concrete is often insufficient while meeting the pervious performance. The lack of strength leads to serious damage and cracking of pervious concrete pavement, and the obvious phenomenon restricts the wide application of pervious concrete pavement. Therefore, it is very important to study the difficulty of the coordination

problem of the permeability coefficient and strength of pervious concrete.

In view of the above difficulties and pain points, many scholars have carried out a large number of studies [4–6]. Xu et al. [7] tested the influence of four different forming methods on the properties of pervious concrete materials, showing that with the increase of vibration time and forming pressure, the mechanical properties of pervious concrete first increased and then decreased. Jiang et al. and Radlińska et al. [8, 9] carried out experiments on the mixing ratio and construction process of pervious concrete and put forward the best design method. Xie et al. [10–12] found that the cement-wrapped stone method of mixing, inserting, and ramming method of molding and the standard curing method were more suitable for the preparation of base material. Nguyen and Sebaibi [13] proposed the screen grouting method, thus obtaining the optimal water-binder ratio of pervious concrete, which is more scientific and practical. Yang and Jiang [14] found that the incorporation of organic polymers can significantly improve the compressive strength of pervious concrete, but the pervious performance is not ideal and the cost is high. Wu et al. [15, 16] carried out research on aggregate particle size, water-cement ratio, water-reducing agent, strengthening agent, and sand ratio on concrete performance, and applied the results to practical projects to improve the service strength of pervious concrete. Guo et al. [17] studied the water permeability, wear resistance, and mechanical properties of pervious concrete with different polypropylene fiber and carbon fiber content. Ahmed et al. [18] studied the factors influencing the performance of steel fiber-reinforced concrete under uniform load. Wang et al. [19] studied that the changes in the strength and permeability coefficient of pervious concrete mixed with steel slag were improved. Yin et al, Qiao et al., and Zhao et al. [20–22] studied the internal pore structure and crack failure characteristics of pervious concrete specimens by microscopic means. Xie et al. [23] studied the incorporation of basalt fibers into concrete and carried out an experimental study on the fatigue behavior of the bond interface under a bending load. Nagajothi et al. [24] studied the cracking behavior of glass fiber and basalt fiber-reinforced concrete under cyclic loading. Hasan Dilbas, Ali Sadrmomtazi, et al. [25, 26] studied the microscopic mechanism of basalt fiber-reinforced concrete by scanning electron microscopy. Rathod et al. [27] conducted experimental research on mixed basalt fiber concrete and ordinary concrete and concluded that basalt fiber concrete has great potential as an alternative construction material.

Basalt fiber is a kind of environmental protection material, with high tensile strength, acid and alkali resistance, outstanding temperature resistance, etc. At home and abroad the incorporation of basalt fiber into concrete to carry out a lot of experimental research and theoretical analysis. The results show that the strength, impermeability, and frost resistance of basalt fiber-reinforced concrete are better than those of ordinary concrete. However, there are still few studies on the incorporation of basalt fiber into pervious concrete at home and abroad, especially the comprehensive analysis of all the incorporation indexes of basalt fiber is even less, and there is also no systematic analysis method that comprehensively considers the diameter, length, and dosage of basalt fiber to determine the optimal incorporation index of basalt fiber.

Given this background, this study incorporated basalt fiber into pervious concrete and proposed a new analysis method-entropy method. The objective is to obtain the optimal incorporation index of basalt fiber to improve the strength of pervious concrete under the premise of ensuring its pervious capacity. The entropy method [25–27] can comprehensively consider the interaction between various indicators, effectively solve the interference caused by the interaction between various factors on the results, and then select the optimal incorporation index. In this study, various indicators of basalt fiber incorporation (diameter, length, and content) were comprehensively considered through the entropy method and combined with the microstructure image, the influence law of different basalt fiber incorporation indexes on the performance of pervious concrete is studied, and the internal mechanism of basalt fiber improving pervious concrete is analyzed. Finally, the best mixing index of basalt fiber is obtained, which can make the mechanical properties and water permeability of pervious concrete optimal at the same time, which provides a reference value for the popularization and application of basalt fiber pervious concrete in practical engineering.

2. Experimental Materials and Methods

2.1. Experimental Materials

2.1.1. Cement. P.O42.5 ordinary Portland cement was used in the experiment. The main chemical components are limestone, clay, and iron ore powder. Its density is 3.1 g/cm^3 and its specific surface area is 380 m^3/kg. The 3-day compressive strength is 25.2 MPa and the 3-day flexural strength is 5.4 MPa. The initial setting time was 225 min and the final setting time was 275 min.

2.1.2. Coarse Aggregate. Single-graded ordinary crushed stone with a 5–10 mm particle size was selected. The compact packing density is 1670 kg/m^3, the apparent density is 2990 kg/m^3, and the packing porosity is 44.15%.

2.1.3. Basalt Fiber. The basalt fiber diameters used in this experiment were 14 μm, 15 μm, 17 μm, and 20 μm, respectively. The length is 12 mm, 15 mm, 18 mm, and 24 mm, respectively. The dosage is 2 kg/m^3, 4 kg/m^3, and 6 kg/m^3, respectively. The raw materials are shown in Figures 1 and 2 and their properties are shown in Table 1.

2.1.4. Silica Fume. The chemical composition of the silica fume selected in this experiment is shown in Table 2.

2.1.5. Water-Reducing Agent. Polycarboxylic acid series high-efficiency water-reducing agent was selected in this experiment. Its properties are a water reduction rate of 37%, a bleeding rate of 40%, and a gas content of 2%.

Figure 1: Chopped basalt fiber.

Figure 2: Microscopic view of chopped basalt fiber.

Table 1: Basalt fiber performance index.

Density (g/cm^3)	Tensile strength (MPa)	Elastic modulus (GPa)	Fracture elongation (%)
2.65	3300–4500	95–115	2.4–3.0

Table 2: Chemical composition of silica fume.

Chemical composition	SiO_2	Al_2O_3	Fe_3O_4	MgO	CaO	Na_2O
Content (%)	96.74	0.32	0.08	0.1	0.11	0.09

2.2. Experimental Method

2.2.1. Experiment Preparation. In the process of making the test piece, the mixing ratio is calculated according to the calculation method in the industry standard "Technical Regulations for Permeable Concrete Pavement (Draft for Partial Revision Provisions)" revised by the Ministry of Housing and Urban-Rural Development in December 2020, in which [4] the water-binder ratio is 0.3 and the design porosity is 15%, the content of silica fume is 5% of the cementitious material, and the content of water-reducing agent is 0.5% of the cementitious material, and calculate the base fit as shown in Table 3. Among them, when the diameter of basalt fiber is used as a variable, the basalt fiber length and content are selected as 12 mm and 2 kg/m^3, respectively. When the basalt fiber length is used as a variable, the basalt fiber diameter and content are 15 μm and 2 kg/m^3, respectively. When the amount is used as a variable, the diameter and length of basalt fibers are selected as 15 μm and 24 mm, respectively.

According to the investigation in literature [28–30], it can be seen that the mixing of basalt fiber permeable concrete not only needs to meet the good mixing state but also needs to ensure the uniform dispersion of the fiber, so it is very important to select an appropriate mixing method. At present, there are three main mixing methods of pervious concrete, which are the one-time feeding method, the cement net slurry method, and the cement stone wrapping method. Compared with the three mixing methods, the cement stone wrapping method is the most complicated process, it is the aggregate and fiber into the blender and stir for 30 s, and then add 20% water and stir for 30 s, followed by adding cement, silica fume, water reducer and the remaining 80% of water, for mixing 150 s to get the mixing material. However, this method is more conducive to uniform fiber dispersion, and can also make the cement slurry fully wrap the aggregate, effectively increasing the bond between the aggregate, thus improving the strength of the permeable concrete. Therefore, a cement-wrapped stone method is used in this research. The equipment and process used in the experiment are shown in Figures 3 and 4.

As there is no fine aggregate inside the pervious concrete, the pores between the aggregate are large and the fluidity of the mixture is poor. The cohesive force of the cement slurry directly affects the strength of the permeable concrete. Therefore, it is also crucial to select the appropriate molding way. At present, there are three main forming methods for permeable concrete indoors: insert-tamping method, vibration forming method, and pressure forming method. The manual tamping method is to put the concrete material into the test mold in three layers. Each layer needs to be tamped from the surrounding to the center with a tamping rod, and the insertion depth should reach 20 mm, this method has good uniformity, but the compressive strength is often not up to the requirements. The vibration molding method in the operation is simple, one only needs to put the concrete into the trial mold at one time, then put it on the vibrating table to vibrate and then remove it, roll it with Φ40 mm steel bar and smooth it with a spatula, but this method has higher requirements on vibration time. If the vibration time is too long, the phenomenon of segregation and back-sealing will occur. If the vibration time is insufficient, the pores will be larger and the strength will be reduced. The pressure forming method is to use special instruments and special steel die for concrete forming, the operation of this method is complex, and has high requirements for experimental equipment. Therefore, after repeated testing, this paper adopts the combination of manual tamping molding and vibration molding. After completion of the parts, the test piece needs to be covered with plastic film and demoulded after 48 hours. After demoulding, the specimen shall be placed into the standard curing room for maintenance and subsequent experiments, as shown in Figures 5 and 6. In order to reduce the experimental error, each observation index of each group of experiments by the average value of three specimens is given as the final experimental result.

2.2.2. Mechanical Properties Test

(1) Compressive Strength Test. According to the "Standard for Test Methods of Physical and Mechanical Properties of Concrete" (GB/T 50081-2019) [31], the compressive strength tests of permeable concrete with different basalt fiber incorporation indexes were carried out, respectively. The compressive strength is tested by a microcomputer-controlled electro-hydraulic servo hydraulic press, as shown in Figure 7. First, turn on the testing machine equipment, place the test piece in the middle of the lower plate of the testing machine, and adjust the upper pressing plate to just touch the upper surface of the test piece. After the specimens are adjusted, turn on the electro-hydraulic servo system to set the parameters, the loading method is selected as load-displacement, the rate is adjusted to 5000 N/s, and the test results of the nonstandard cubic concrete specimens with the size of 100 mm × 100 mm × 100 mm should be multiplied by the coefficient of 0.95. After adjusting the parameters, manually click the equipment start button to start the test. Click the stop button when the specimen's sharp deformation reaches necking failure, and record the failure load F. The compressive strength of specimens was calculated according to the following formula:

$$f = \frac{F}{A}, \tag{1}$$

where f—compressive strength of the specimen, MPa. F—maximum load of the specimen, N. A—the loading area of the specimen, mm^2.

(2) Split Tensile Strength Test. The splitting tensile strength of basalt fiber permeable concrete was measured according to the "Standard for Test Methods of Physical and Mechanical Properties of Concrete" (GB/T 50081-2019) [31]. The microcomputer-controlled electro-hydraulic servo hydraulic press is still used for the splitting tensile strength test. The test device is shown in Figure 8. First, open the testing

Table 3: mixture ratio of ordinary permeable concrete.

Aggregate (kg/m^3)	Water (kg/m^3)	Silica fume (kg/m^3)	Cement (kg/m^3)	Water-reducing agent (kg/m^3)
1636.6	144.32	24.05	457.02	2.41

Figure 3: Concrete mixer diagram.

Figure 5: Sprinkling maintenance diagram of the cover film of the test piece.

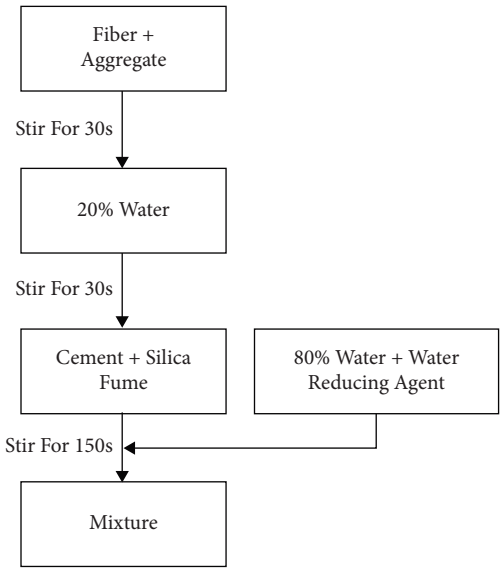

Figure 4: Flow chart of cement-wrapped stone method.

Figure 6: Conservation diagram of specimen curing room.

machine equipment, install a pad block between the upper and lower pressure plates of the testing machine, and then put the specimen into the center of the pad block, that is, the center line of the specimen is recombined with the central axis of the pad block, and the upper-pressure plate is adjusted to the position exactly in contact with the upper surface of the test block. After the specimens were adjusted, turn on the electro-hydraulic servo system to set the parameters, select load displacement for the loading method, and select 500 N/s for the rate. In addition, nonstandard cubic concrete specimens with specimen size of 100 mm × 100 mm × 100 mm were used in this test. According to the specification [28], the test result should be multiplied by a coefficient of 0.85. After the parameters are adjusted, start the test, manually click the equipment start

Figure 7: experimental device of compressive strength.

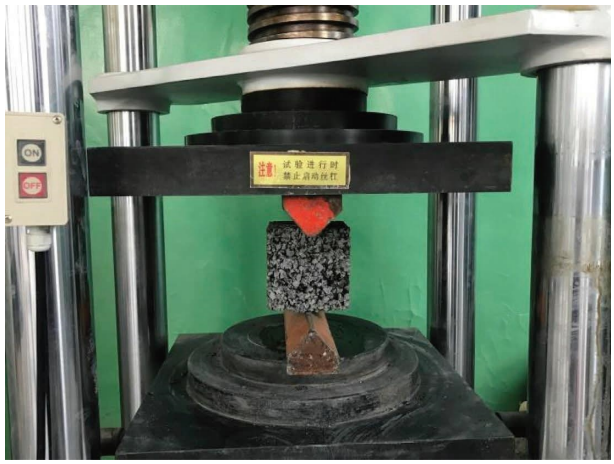

Figure 8: Split tensile test device.

button, click the stop button, and record the failure load F when the specimen's sharp deformation reaches necking failure. The splitting tensile strength of specimens is calculated according to the following formula:

$$f = \frac{2F}{\pi A} = 0.637\frac{F}{A}, \tag{2}$$

where f—specimen splitting tensile strength, MPa; F—maximum load of a specimen, N; A—the loading area of the specimen, mm^2.

2.2.3. Water Permeability Test

(1) Porosity Test. The continuous porosity of basalt fiber permeable concrete was measured according to "Technical Specification for Permeable Concrete Pavement (Draft of Partial Revision)" [32]. First, take out the 28-day-old specimen from the curing room, the specimen was immersed in water from 15°C to 25°C, and make sure the water is higher than on the specimen surface by more than 20 mm. After one day, take it out to dry, and then put the specimen into the bucket, and the bucket is placed above the balance, and the suspended mass m_1 (accurate to 1 g) of the test piece in the water is weighed, as shown in Figure 9, and finally the test piece is taken out and drained. When there is no water dripping at the bottom of the specimen, the mass m_2 of the specimen (accurate to 1 g) is weighed, and the continuous porosity of the pervious cement concrete specimen is calculated according to the following formula:

$$K_r = \left(1 - \frac{m_2 - m_1}{\rho_w V}\right) \times 100, \tag{3}$$

where K_r—continuous porosity of the specimen, %; m_1—suspension immersion mass of the specimen, kg; m_2—the mass of the dry state of the saturated surface of the specimen, kg; ρ_w—density of water, kg/m^3; V—specimen volume, m^3.

(2) Water Permeability Coefficient Test. Referring to the "Technical Specification for Pervious Concrete Pavement (Draft for Comments on Partial Revision Provisions)" [32], this paper adopts the fixed water head method to test the permeability coefficient of permeable concrete with different basalt fiber incorporation indexes. Firstly, a specimen of 28-day-old was taken out of the curing chamber and immersed in water for 24 hours to make it saturated with water absorption. After 24 hours, take out the specimen, spread it evenly around the specimen with cement mortar, and dry it to ensure that the water only penetrates through the upper and lower surfaces of the see-through concrete, then put the blocked specimen into the measuring cylinder of the water inlet, and seal the connection between the measuring cylinder and the test block with plasticine, and conduct the water permeability test after sealing. During the test, water should be continuously injected into the overflow tank. After the overflow hole of the overflow tank starts to emit water, the water injection should be stopped immediately. After the water flow velocity of the overflow hole of the overflow tank becomes stable, start to measure the amount of water flowing out of the overflow hole within five minutes. The experimental device is shown in Figure 10, and calculate the water permeability coefficient according to the following formula:

$$K_T = \frac{D}{h_0} \times \frac{Q}{A_0 \times T}, \tag{4}$$

where K_T—water permeability coefficient at T°C, cm/s; D—specimen thickness, cm; Q—time is the amount of water passing through the specimen at time "T," kg; A_0—specimen area, cm^2; h_0—head height, cm; T—test time, s.

3. Experimental Results and Analysis

3.1. Analysis of Influencing Factors of Basalt Fiber Diameter on Performance of Pervious Concrete. According to "Technical Regulations for Permeable Cement Concrete Pavement" CJJ/T 135-2009 [33], the standard value of compressive strength of C20 pervious cement concrete is 20 MPa, the standard value of splitting tensile strength is 2.5 MPa, the target porosity is 15%, and the standard value of permeability coefficient is 0.5 mm/s. It can be seen from Table 4 that the addition of basalt fiber significantly improves the mechanical properties of permeable concrete. However, the permeability of pervious concrete is inhibited to a certain

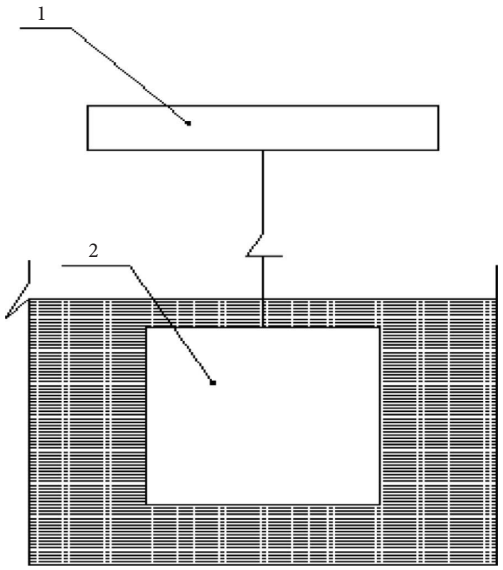

Figure 9: Experimental device for porosity measurement. (Note: 1-electronic balance, 2-permeable concrete test block).

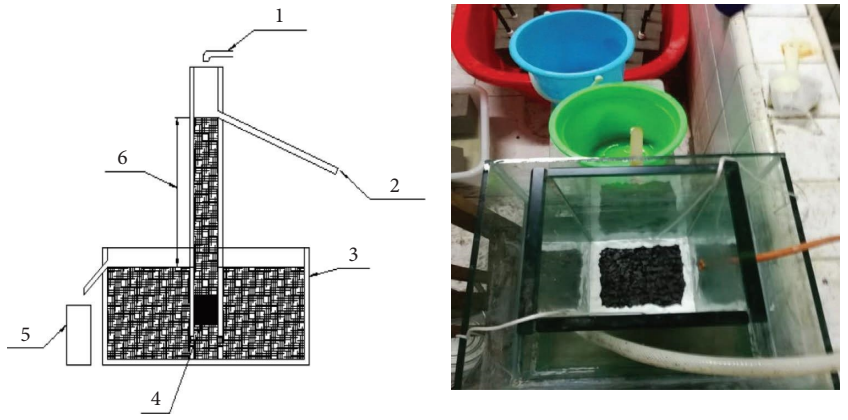

(a) (b)

Figure 10: Experimental advice of fixed head method. (Note: 1-water supply system, 2-overflow pipe, 3-flow trough, 4-pervious concrete test block, 5-measuring cylinder, and 6-water level difference).

Table 4: Test results of pervious concrete with different basalt fiber diameters.

Group	Fiber diameter (μm)	Fiber lengths (mm)	Fiber content (kg/m^3)	Compressiv strength (MPa)	Splitting tensile strength (MPa)	Porosity (%)	Permeable coefficient (mm/s)
0	—	—	—	19.51	2.73	17.42	6.81
1	14	12	2	24.11	3.48	14.93	2.98
2	15	12	2	23.13	3.52	15.16	3.19
3	17	12	2	21.85	3.74	15.24	3.60
4	20	12	2	19.82	2.99	15.31	4.43

extent, which is due to the pores in pervious concrete are filled with fibers, which increases the degree of compactness of the specimen, leading to a decrease of the water permeability of the pervious concrete, but it still meets the requirements of the specification value on the whole.

According to the performance test results of permeable concrete with different basalt fiber diameters, a broken line chart of the effect of different diameters of basalt fibers on the mechanical properties and water permeability of pervious concrete is drawn, as shown in Figure 11. The microstructure images of the interface between basalt fiber with different diameters and cement base in Figure 12 are obtained by 【Phenom】 Scanning Electron Microscopy. It can be seen from Figure 11(a) that with the increase of basalt

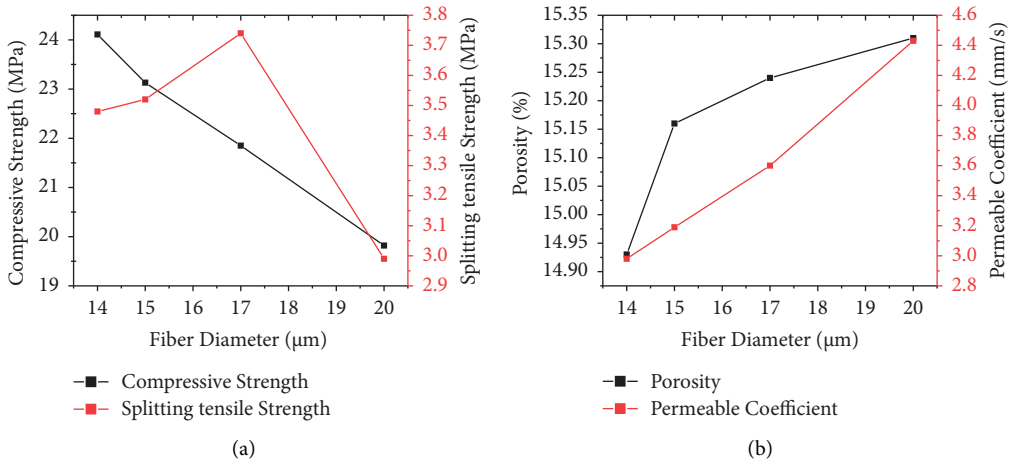

Figure 11: Line chart of influence of different basalt fiber diameters on pervious concrete properties. (a) Relationship between fiber diameter and mechanical properties. (b) Relationship between fiber diameter and water permeability.

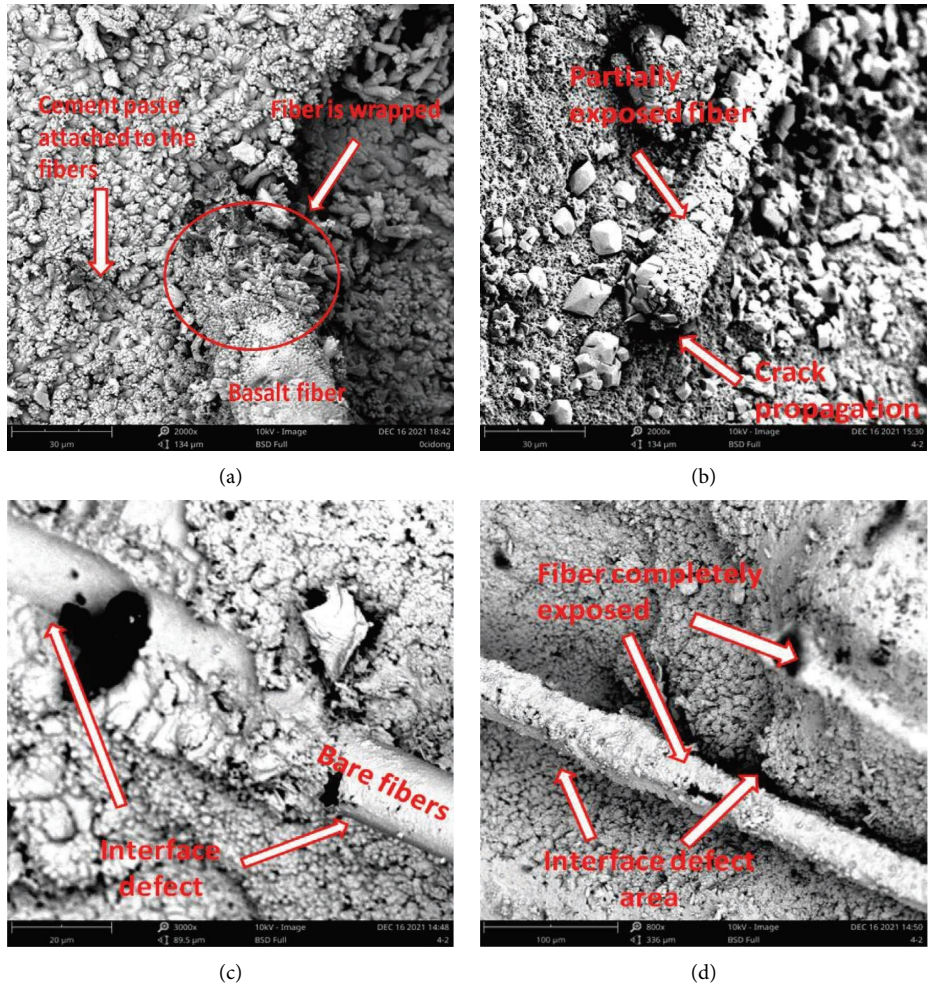

Figure 12: Microstructure of fiber-cement-based interface with different diameters. (a) Microstructure of 14 μm fiber-cement base interface. (b) Microstructure of 15 μm fiber-cement base interface. (c) Microstructure of 17 μm fiber-cement base interface. (d) Microstructure of 20 μm fiber-cement base interface.

fiber diameter, the compressive strength of pervious concrete decreases continuously. When the fiber diameter is 14 μm, the compressive strength is the largest, and its value is 24.11 MPa. When the fiber diameter increases to 20 μm, the compressive strength decreases to 19.82 MPa. The reason is that when the diameter of the basalt fiber increases if its surface area is larger, the encapsulation of the cement slurry will be more unfavorable. It can be clearly seen from Figure 12(a) that the fibers with a diameter of 14 μm can be closely combined with the cement matrix, and the surface of the fibers is covered with a thick layer of cementitious material, which can strengthen the bonding ability between the fibers and the cement matrix interface. From Figures 12(b)–12(d), the fibers with diameters of 15 μm, 17 μm, and 20 μm, respectively, are not ideally wrapped with the cement slurry. When the diameter is too large, the fibers are even completely exposed. It not only loses the function of the fiber but also reduces the contact area between the aggregate and the cement paste, forming more interface defect areas inside the concrete, resulting in the reduction of the bond between aggregate and cement slurry, thereby reducing the compressive strength of basalt fiber pervious concrete. As shown in Figure 11(a), the split tensile strength of pervious concrete increases first and then decreases with the increase of basalt fiber diameter. When the fiber diameter is 17 μm, the maximum split tensile strength of pervious concrete reaches 3.74 MPa. According to Figures 12(b) and 12(c), it can be seen that the reason why the splitting tensile strength increases first is that when the fiber diameter is too small and under the action of external force, the tensile effect of the fiber is pulled out before it comes into play, while the tensile effect of the fiber with a slightly larger diameter is obvious, so the splitting tensile strength tends to increase first. Along with the fiber, the diameter continues to increase, the splitting tensile strength of the permeable concrete begins to show a downward trend, the principle is similar to the compressive strength, mainly because when the fiber diameter is too large, and the interface defect area inside the permeable concrete is increased, which affects the bonding force between the aggregate and the cement paste, thereby reducing the splitting tensile strength of the pervious concrete. It can be seen from Figure 11(b) that the porosity and permeability coefficient of pervious concrete show a rising trend with the increase of basalt fiber diameter, and both are optimal at 20 μm. This is due to the increase in fiber diameter, resulting in a reduction in the number of fibers per unit volume, thus improving the permeability of basalt fiber permeable concrete.

3.2. Analysis of Influence Factors of Basalt Fiber Length on Properties of Pervious Concrete. The experimental results of mechanical properties and water permeability of permeable concrete with different basalt fiber lengths are shown in Table 5. The broken line diagram of the effect of different lengths of basalt fibers on the mechanical properties and water permeability of pervious concrete is shown in Figure 13. The SEM microstructure of the interface between basalt fiber with different lengths and cement base is shown in Figure 14. In terms of mechanical strength, the compressive strength of the fiber with a length of 24 mm is the best, which is 20.54% higher than that of the fiber with a length of 12 mm. Investigate the reason, with the change in the basalt fiber length, the permeable concrete will not be destroyed quickly once cracks appear when a permeable concrete ultimate load is reached. Because it can through the cross crack and the stress is not easy to be pulled out of fiber function make concrete internal stress redistribution, and transform the development path of the cracks, preventing the cracks from developing and penetrating, thereby improving the compressive strength, as shown in Figure 14(a). At the same time, previous studies [6, 34, 35] have shown that basalt fibers of appropriate length are uniformly dispersed in the permeable concrete matrix, and the formed three-dimensional framework can inhibit aggregate settlement, reduce the shrinkage and deformation of the matrix, and significantly improve the compressive strength of concrete.

For the splitting tensile strength of pervious concrete, the splitting tensile strength increases first and then decreases with the increase of basalt fiber length, and the splitting tensile strength is the best at 18 mm, which increases by 12.08% compared with 15 mm fiber. This is because the internal structure of permeable concrete under the action of load will be damaged, and microcracks will appear at the interface, resulting in the phenomenon of falling off between the cementitious material and the aggregate. As the load continues to increase, microcracks develop and form microcracks. At this time, the basalt fibers with a slightly longer length and not easy to be pulled out mixed into the permeable concrete can replace the concrete and resist the rapid development of internal cracks in the permeable concrete. Until the final load exceeds the fiber bearing capacity, the fiber is pulled off, and the test block completely loses its bearing capacity, as shown in Figures 14(b) and 14(c). As the fiber length continued to increase, the splitting tensile strength decreased, and the splitting tensile strength of the fiber with a length of 24 mm decreased by 14.9% compared with the fiber with a length of 18 mm. The reason for this phenomenon is that the fibers with too long lengths are more likely to be broken during the concrete mixing process, as shown in Figure 14(d). It is difficult for the broken fiber to effectively transmit the load to both sides of the crack when subjected to an external force. Therefore, if the fiber is too long, it cannot play a significant role but lead to a decrease in the splitting tensile strength.

It can be seen from Figure 13(b) that with the increase of basalt fiber length, both the porosity and permeability coefficient of pervious concrete show a rising trend. When the length of basalt fiber is 24 mm, the pervious concrete shows the best permeability, the porosity is 16.13% and the permeability coefficient is 5.03 mm/s at this time. Compared with the length of basalt fiber is 18 mm, the porosity and water permeability increased by 1.38% and 8.41%, respectively. The reason for this phenomenon is similar to the principle of changing the diameter of basalt fibers. As the length of basalt fibers increases, the number of fibers

Table 5: Test results of pervious concrete with different basalt fiber lengths.

Group	Fiber lengths (mm)	Fiber diameter (μm)	Fiber content (kg/m^3)	Compressive strength (MPa)	Splitting tensile strength (MPa)	Porosity (%)	Permeable coefficient (mm/s)
0	—	—	—	19.51	2.73	17.42	6.81
1	12	15	2	23.13	3.52	15.16	3.19
2	15	15	2	24.63	3.89	15.68	3.63
3	18	15	2	25.74	4.36	15.91	4.64
4	24	15	2	27.88	3.71	16.13	5.03

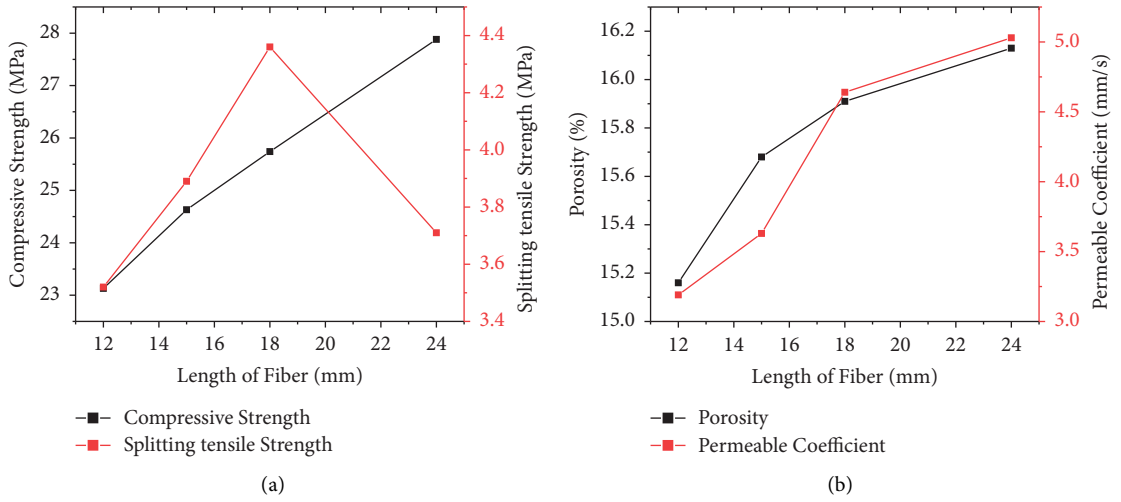

Figure 13: Broken line diagram of influence of different basalt fiber lengths on pervious concrete properties. (a) Relationship between fiber length and mechanical properties. (b) Relationship between fiber length and water permeability.

required per unit volume will decrease, and the chance of blocking pores will be smaller. In addition, the long fibers are easy to disperse into a network inside the specimen, which increases the permeable area and facilitates the passage of water molecules. This leads to an increase in the porosity and water permeability coefficient of pervious concrete.

3.3. Analysis of Influence Factors of Basalt Fiber Content on Pervious Concrete Performance. Table 6 shows the experimental results of the mechanical properties and water permeability of permeable concrete with different content of basalt fiber. According to the experimental results, the broken line charts of the influence of different basalt fiber content on the mechanical properties and water permeability of pervious concrete are drawn, as shown in Figure 15. The microstructural diagram of the interface between basalt fiber with different contents and cement base is obtained by 【Phenom】 scanning electron microscopy, as shown in Figure 16. From the experimental results, it can be concluded that with the increase in basalt fiber content, the compressive strength of permeable concrete shows a downward trend. When the content of basalt fiber is 2 kg/m^3, the best compressive strength is obtained, which is higher than the content of 4 kg/m^3 increased by 11.30%, which is 19.4% higher than that of 6 kg/m^3. This is due to an appropriate amount of basalt fibers being evenly dispersed inside the pervious concrete matrix, and the formed three-dimensional skeleton effectively inhibits the settlement of aggregates and reduces the shrinkage deformation of the matrix, as shown in Figure 16(a), when the chopped basalt fibers with an appropriate dosage of mixed into concrete, the concrete compressive strength can be improved significantly. However, with the increase of the basalt fiber content, some fibers are easy to clump, as shown in Figure 16(c), so that new defects are formed inside the pervious concrete, which will have a detrimental effect on the mechanical properties of the concrete. Therefore, the compressive strength of basalt fiber pervious concrete showed a downward trend with the increase in fiber content. In contrast, in Figure 15(a), the splitting tensile strength shows an upward trend. The optimal splitting tensile strength was obtained when the basalt fiber content was 6 kg/m^3, and the splitting tensile strength can reach 4.59 MPa at this time. The reason is that during the loading process of the permeable concrete cube splitting tensile test block, the microcracks inside the concrete matrix develop slowly under the load. With the increase in load, the microcracks develop into cracks and connect to form visible cracks. When there are enough cracks, a failure surface is formed and the test block loses its bearing capacity. However, a large number of basalt fibers distributed evenly and randomly in the pervious concrete matrix can effectively inhibit the stress concentration phenomenon at the crack tip, delay the formation of weak surfaces, and improve the splitting tensile strength of basalt fiber pervious concrete.

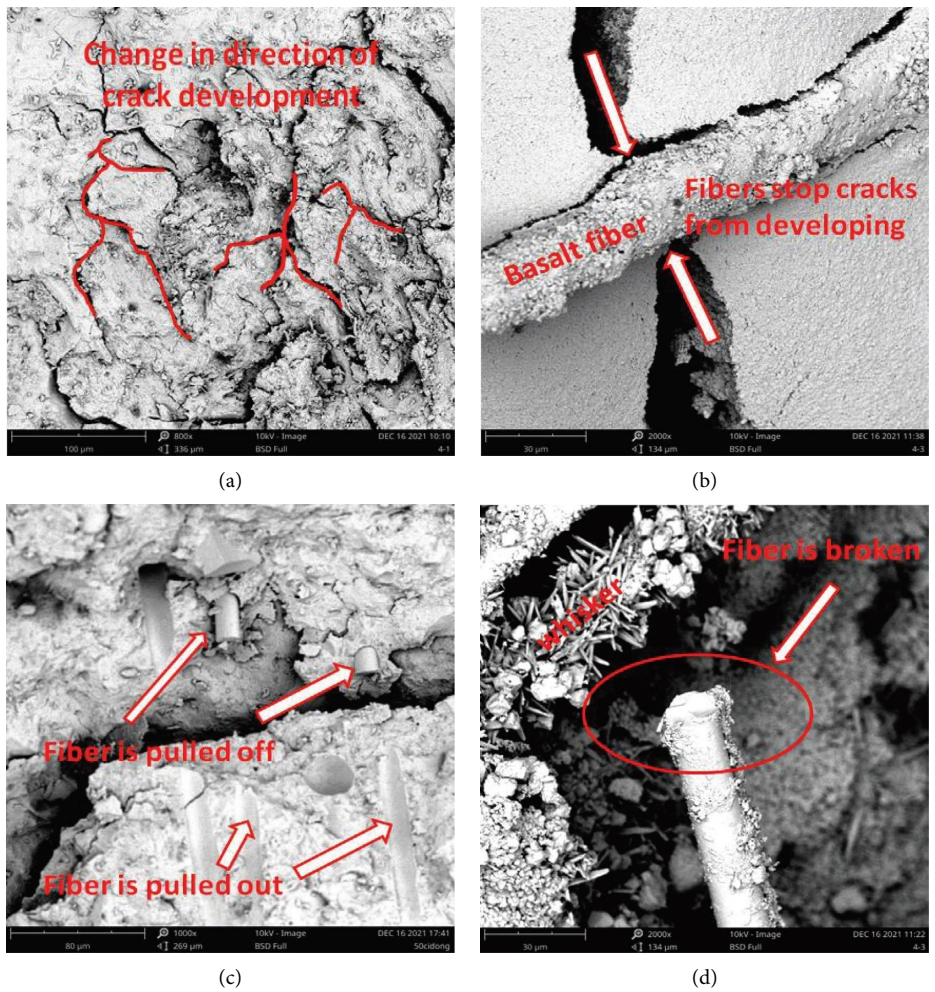

Figure 14: Microstructure of fiber-cement interface with different lengths. (a) Fibers change the direction of fracture development. (b) Fibers are stressed to resist crack development. (c) The fibers are strained and pulled apart. (d) The fibers are interrupted during the mixing process.

Table 6: Test results of pervious concrete with different content of basalt fiber.

Group	Fiber content (kg/m^3)	Fiber diameter (μm)	Fiber lengths (mm)	Compressive strength (MPa)	Splitting tensile strength (MPa)	Porosity (%)	Permeable coefficient (mm/s)
0	—	—	—	19.51	2.73	17.42	6.81
1	2	15	24	27.88	3.71	16.13	5.03
2	4	15	24	25.05	4.18	15.69	4.02
3	6	15	24	23.35	4.59	14.88	3.05

Studies [36–38] have shown that the additional amount of basalt fibers not only affects the mechanical properties of permeable concrete but also affects its water permeability to a certain extent. It can be seen from the experimental results that when the basalt fiber content is 2 kg/m^3, the maximum porosity is obtained, which is 16.13%. When the fiber content increases to 4 kg/m^3, the porosity decreases by 0.44%. When the fiber content continued to increase to 6 kg/m^3, it decreased again by 0.81% compared with the content of 4 kg/m^3. This is because pervious concrete is composed of connected pores, semiconnected pores, and closed pores. The addition of fiber will enter connected pores and semiconnected pores, resulting in an increase in the number of closed pores, resulting in a decrease in porosity. Similarly, when the content of basalt fiber is 2 kg/m^3, the optimal water permeability coefficient can be obtained, and the water permeability coefficient value is 5.03 mm/s at this time. When the fiber content increased to 4 kg/m^3, the water permeability decreased by 25.12%. When the fiber content increased to 6 kg/m^3, it decreased by 31.8% compared with the content of 4 kg/m^3. Analysis of the reasons shows that too many fibers will agglomerate and block the pores in the

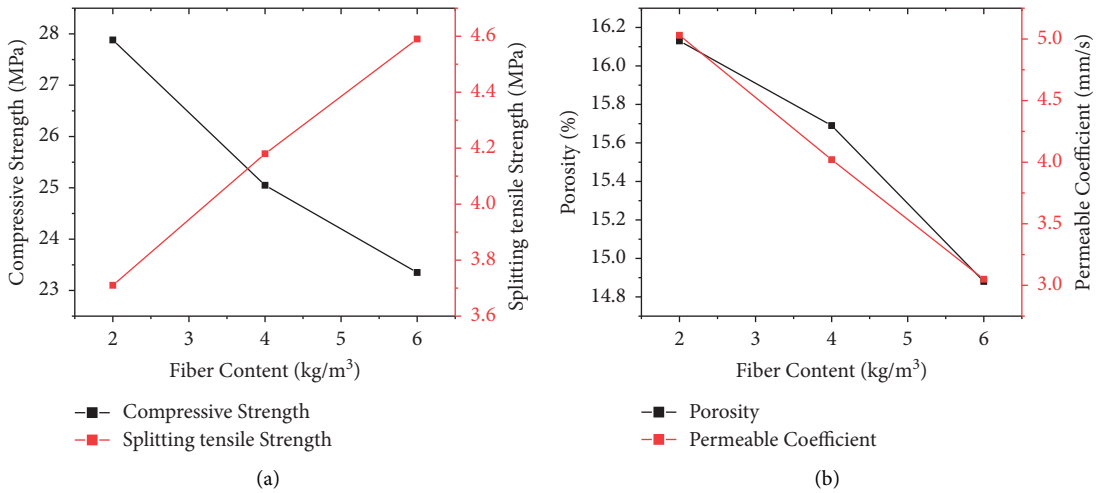

Figure 15: Line chart of influence of different content of basalt fiber on performance of pervious concrete. (a) Relationship between fiber content and mechanical properties. (b) Relationship between fiber content and water permeability.

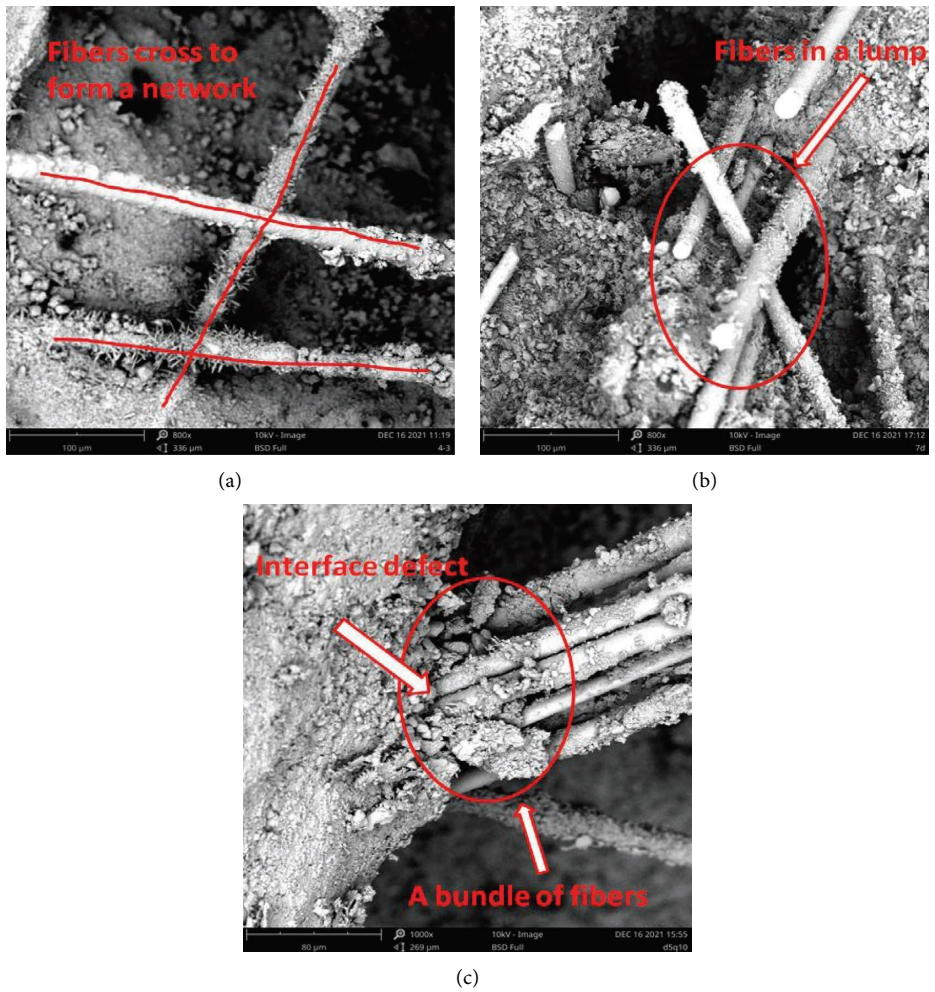

Figure 16: Microstructure of fiber-cement-based interface with different dosages. (a) Microcosmic diagram of fiber-cement base interface with 2 kg/m^3 dosage. (b) Microcosmic diagram of fiber-cement base interface with 4 kg/m^3 dosage. (c) Microcosmic diagram of fiber-cement base interface with 6 kg/m^3 dosage.

pervious concrete, resulting in an increase in the number of closed pores and a decrease in the water permeability coefficient.

4. Comprehensive Evaluation and Analysis by Entropy Method

In chapter 3, the compressive strength, splitting tensile strength, porosity, and permeability coefficient of pervious concrete with different basalt fiber diameters, lengths, and dosages have been obtained through experiments, and the reasons for the change in pervious concrete performance caused by these different incorporation indicators have been analyzed and discussed. However, based on these analyses, we cannot select an incorporation index that optimizes both mechanical properties and water permeability. Therefore, it is necessary to select a systematic method to evaluate the influence of various factors on the performance of permeable concrete and analyze which performance index has the greatest impact and the highest contribution rate in pervious concrete, thus determining the optimal incorporation index of each factor of basalt fiber. Thus, the method—entropy method, commonly used in the field of sustainable development evaluation and social economics is applied in this chapter, which can comprehensively consider the interaction between various indicators and effectively solve the deviation caused by the interaction of various factors on the results, so as to select the basalt fiber incorporation index that can achieve the optimal mechanical properties and water permeability.

4.1. Entropy Analysis Theory and Method. The key to evaluating a model lies in the determination of the index weight. The determination of the index weight can be mainly divided into two methods: subjective weighting and objective weighting. Common subjective weighting methods include Analytic Hierarchy Process (AHP), and the Delphi method. The objective weighting includes multivariate statistical methods, and entropy methods, which have their applicability under different application requirements [39, 40]. The entropy method, originally derived from the concept of thermodynamics in physics, is an objective method to determine the weight of each indicator. It mainly uses the physical calculation formula to measure the uncertainty of information to determine its weight, and then comprehensively analyzes each evaluation object [41–43]. Generally, if the entropy is higher and the data is more chaotic, its utility value will be smaller and the weight will be smaller. If the entropy value is smaller, the final weight will be larger [44]. In addition, the evaluation index calculated by the entropy method is a relative value, so this method is widely used in the relative evaluation of multiple indicators [45, 46]. And this experiment is just right to have multiple evaluation indexes of compressive strength, splitting tensile strength, porosity, and permeability coefficient, using the entropy method just can solve the problem that the sensitivity of different basalt fiber diameter, length, and dosage factors to the evaluation index is not clear, but also can solve the factors influence each other, avoid subjective interference. It shows that the method is reasonable and effective in this experiment. In addition, in the third chapter, this paper has obtained the compressive strength, split tensile strength, porosity, and permeability coefficient of pervious concrete under different basalt fiber diameters, lengths, and dosages through experiments. The experimental data are accurate and complete, creating necessary conditions for choosing the entropy method.

The calculation steps of the entropy method are as follows:

(1) The dimensionless processing of data is the first step in entropy evaluation. Since the entropy value method determines the weight of the index according to the difference between the data, the entropy value method has higher requirements for dimensionless data. However, studies [47] have shown that the dimensionless processing of data will make the difference between the original indicators change to a certain extent. Under feasible conditions, the entropy method is used to calculate the weight of each indicator based on the original data rather than the dimensionless data, which can make better use of the differences shown by the original data. Therefore, this paper uses the original data to calculate the weight of each indicator.

(2) Calculate the proportion of the j-th influencing factor index of the i-th performance index. Assuming that there are "m" measurement performances forming the object set $\{M_i\}$ ($i = 1, 2, \ldots, m$), and there are "n" influencing factor indicators forming the index set $\{C_j\}$ ($j = 1, 2, \ldots, n$). Among them, X_{ij} represents the original value of the j-th influencing factor index of the i-th measurement performance. A standard matrix R composed of the proportion ξ_{ij} of different values in different indicators is obtained after normalization according to the following equations:

$$\% \ \xi_{ij} = \frac{X_{ij}}{\sum_{i=1}^{m} X_{ij}} \ (\mathrm{i} = 1, 2, 3 \ldots\ldots \mathrm{m}, \mathrm{j} = 1, 2, 3 \ldots\ldots \mathrm{n}), \tag{5}$$

$$R_{ij} = \begin{bmatrix} & M_1 & M_2 & \cdots & M_m \\ C_1 & \xi_{11} & \xi_{21} & \cdots & \xi_{m1} \\ C_2 & \xi_{12} & \xi_{22} & \cdots & \xi_{m2} \\ \vdots & \vdots & \vdots & \cdots & \vdots \\ C_n & \xi_{1n} & \xi_{2n} & \cdots & \xi_{mn} \end{bmatrix}. \tag{6}$$

(3) Calculate the entropy value of each index. After the standardized data matrix is obtained, a comprehensive analysis can be carried out. According to the calculation of the following formula, the entropy value e_j of each evaluation index can be obtained.

$$e_j = -\mathrm{K}\sum_{i=1}^{m}\xi_{ij}\ln\xi_{ij}, \tag{7}$$

where $e_j \in (0, 1)$. K is a constant, that is, $K = 1/\ln m$, which is related to the sample number "m" of the influencing factor index of the system.

(4) It can be seen from formula (7) that when the order degree is 0, the entropy value is the maximum, that is, $e = 1$. Since the entropy value e_j can be used to measure the data utility value of the influence factor index of the j-th item. When m samples are in a completely disordered distribution state, $\xi_{ij} = 1/\mathrm{m}$, the utility value of the entropy value to the comprehensive evaluation is zero at this time. Therefore, the difference coefficient g_j can be defined to describe the discrete degree of the data, which is determined by the difference between the entropy value of this index and 1, as shown in the formula. Among them, the larger the g_j, the greater the influence of the indicator.

$$g_j = 1 - e_j\,(\mathrm{j} = 1, 2, 3 \ldots\ldots \mathrm{n}). \tag{8}$$

(5) Calculate the weight of the j-th indicator according to formula (9).

$$w_j = \frac{g_j}{\sum_{j=1}^{n} g_j}. \tag{9}$$

(6) The product of the j-th evaluation index of the i-th sample in the standardized matrix and the j-th index weight w_j is used as the evaluation index F_i, as shown in formula (10). Obviously, the larger the evaluation index F_i, the better the sample effect, and finally the evaluation conclusion is obtained based on the comparison results of all evaluation indexes.

$$F_i^k = \sum w_j^k \times X_{ij}^k. \tag{10}$$

4.2. Comprehensive Evaluation and Analysis Results of Basalt Fiber Diameter on Pervious Concrete Performance. The length of basalt fiber selected in this experiment is 12 mm, the dosage is 2 kg/m^3, and the diameter is 14 μm, 15 μm, 17 μm, and 20 μm, respectively. Firstly, according to the data in Table 4 in Chapter 3, the standardized matrix of formula (10) is established, as shown in the following formula. Then substitute equations (7)–(9) to obtain the weight of each indicator, as shown in Table 7.

$$R_{ij}\begin{bmatrix} & M_1 & M_2 & M_3 & M_4 \\ C_1 & 0.271 & 0.260 & 0.246 & 0.223 \\ C_2 & 0.253 & 0.256 & 0.272 & 0.218 \\ C_3 & 0.246 & 0.250 & 0.251 & 0.252 \\ C_4 & 0.210 & 0.225 & 0.254 & 0.312 \end{bmatrix}. \tag{11}$$

It can be seen from the index weight table that when only the basalt fiber diameter is changed, the entropy value of the permeability coefficient is the smallest, so it has the greatest influence on the total benefit evaluation of pervious concrete performance, and the contribution degree reaches 66.70%. In the evaluation of total efficiency, the splitting tensile strength takes second place, and the contribution rate is 18.26%, but the contribution rate is quite different from the permeability coefficient, which has the greatest influence on efficiency. The second is the compressive strength, whose contribution rate is not much different from the splitting tensile strength, accounting for 14.79%. Porosity contributes the least to efficiency evaluation and has the smallest weight, accounting for only 0.25%. Then take the product of the j-th evaluation index of the i-th sample in the standardized matrix and the j-th index weight w_j is used as the evaluation index F_i, and the calculation results of the evaluation index for different basalt fiber diameters are obtained according to formula (10) in Table 8.

$$F_i^k = \sum w_j^k \times X_{ij}^k F_i^k = \begin{bmatrix} C_1 & C_2 & C_3 & C_4 \\ 0.148 & 0.182 & 0.003 & 0.667 \end{bmatrix} \times \begin{bmatrix} M_1 & M_2 & M_3 & M_4 \\ 0.271 & 0.260 & 0.246 & 0.223 \\ 0.253 & 0.256 & 0.272 & 0.218 \\ 0.246 & 0.250 & 0.251 & 0.252 \\ 0.210 & 0.225 & 0.254 & 0.312 \end{bmatrix} = \begin{bmatrix} M_1 & M_2 & M_3 & M_4 \\ 0.227 & 0.236 & 0.256 & 0.281 \end{bmatrix}. \tag{12}$$

The evaluation index is the discrimination of the utility value of various performance indicators, which avoids the interference of subjective factors on the evaluation results to a certain extent [48]. From the calculation results of the evaluation index in Table 8, it can be seen that the selection of basalt fiber with a diameter of 20 μm makes the utility value of each performance index reach the optimum, and the evaluation index is 0.281 at this time. Therefore, 20 μm is selected as the optimal incorporation index of the basalt fiber diameter.

4.3. Comprehensive Evaluation and Analysis Results of Basalt Fiber Length on Pervious Concrete Performance. The diameter of basalt fiber selected in the experiment is 15 μm, the dosage is 2 kg/m^3, and the length is 12 mm, 15 mm, 18 mm, and 24 mm, respectively. Firstly, according to the data in

Table 7: Entropy weight calculation results of different basalt fiber diameters.

	Compressive strength C_1	Splitting tensile strength C_2	Porosity C_3	Permeable coefficient C_4
Entropy (e_j)	0.998100	0.997654	0.999968	0.991429
Difference coefficient (g_j)	0.001900	0.002346	0.000032	0.008571
Entropy weight (w_j)	0.147898	0.182560	0.002503	0.667039

Table 8: Calculation results of evaluation index for different basalt fiber diameters.

Fiber diameter (μm)	14	15	17	20
Evaluation index (F_i)	0.227	0.236	0.256	0.281

Table 9: Entropy weight calculation results of different basalt fiber lengths.

	Compressive strength C_1	Splitting tensile strength C_2	Porosity C_3	Permeable coefficient C_4
Entropy (e_j)	0.998323	0.997692	0.999810	0.988207
Difference coefficient (g_j)	0.001677	0.002308	0.000190	0.011793
Entropy weight (w_j)	0.105036	0.144509	0.011919	0.738536

Table 5 in chapter 3, calculation and arrangement are carried out, and the standardized matrix of formula (6) is established, as shown in the formula. Then substitute equations (7)–(9) to obtain the weight of each indicator, as shown in Table 9.

$$R_{ij}\begin{bmatrix} & M_1 & M_2 & M_3 & M_4 \\ C_1 & 0.228 & 0.243 & 0.254 & 0.275 \\ C_2 & 0.227 & 0.251 & 0.282 & 0.240 \\ C_3 & 0.241 & 0.249 & 0.253 & 0.257 \\ C_4 & 0.193 & 0.220 & 0.281 & 0.305 \end{bmatrix}. \quad (13)$$

It can be seen from the above table that in the case of only changing the length of basalt fibers. The order of the entropy value of each performance index is as follows: porosity is greater than compressive strength, greater than splitting tensile strength, and greater than water permeability coefficient, water permeability coefficient is greater than splitting tensile strength, so the weights are greater than compressive strength and greater than the porosity. That is to say, the permeability coefficient has the greatest influence on the overall benefit evaluation of pervious concrete performance, and its contribution to the total efficiency reaches 73.85%. The porosity has the smallest contribution and the smallest weight in the efficiency evaluation, accounting for only 1.19%. Finally, the product of the j-th evaluation index of the i-th sample in the standardized matrix and the j-th index weight w_j is used as the evaluation index F_i, and the calculation results of the evaluation index in Table 10 are obtained by calculating according to formula (10).

$$F_i^k = \sum w_j^k \times X_{ij}^k F_i^k = \begin{bmatrix} C_1 & C_2 & C_3 & C_4 \\ 0.105 & 0.144 & 0.012 & 0.739 \end{bmatrix} \times \begin{bmatrix} M_1 & M_2 & M_3 & M_4 \\ 0.228 & 0.243 & 0.254 & 0.275 \\ 0.227 & 0.251 & 0.282 & 0.240 \\ 0.241 & 0.249 & 0.253 & 0.257 \\ 0.193 & 0.220 & 0.281 & 0.305 \end{bmatrix} = \begin{bmatrix} M_1 & M_2 & M_3 & M_4 \\ 0.203 & 0.227 & 0.278 & 0.292 \end{bmatrix}. \quad (14)$$

It can be seen from the calculation results of the evaluation index in Table 10 that the selection of basalt fiber with a length of 24 mm makes the utility value of each performance index reach the optimum, and the evaluation index is 0.292 at this time. To sum up, 24 mm is selected as the optimal incorporation index of basalt fiber length.

Table 10: Calculation results of evaluation index for different basalt fiber lengths.

Fiber length (mm)	12	15	18	24
Evaluation index (F_i)	0.203	0.227	0.278	0.292

Table 11: Entropy weight calculation results of different basalt fiber contents.

	Compressive strength C_1	Splitting tensile strength C_2	Porosity C_3	Permeable coefficient C_4
Entropy (e_j)	0.997557	0.996586	0.999495	0.981560
Difference coefficient (g_j)	0.002443	0.003414	0.000505	0.018440
Entropy weight (w_j)	0.098504	0.137655	0.020379	0.743461

Table 12: Calculation results of evaluation index for different basalt fiber contents.

Fiber content (kg/m^3)	2	4	6
Evaluation index (F_i)	0.393	0.332	0.275

4.4. Comprehensive Evaluation and Analysis Results of Basalt Fiber Content on Pervious Concrete Performance. The diameter of the basalt fiber selected in this experiment is 15 μm, the length is 24 mm, and the dosage is 2 kg/m^3, 4 kg/m^3, and 6 kg/m^3, respectively. Firstly, according to the data in Table 6 in chapter 3, calculation and arrangement are carried out, and the standardized matrix of formula (6) is established, as shown in the formula. Then substitute equations (7)–(9) to obtain the weight of each indicator, as shown in Table 11.

$$R_{ij} = \begin{bmatrix} & M_1 & M_2 & M_3 \\ C_1 & 0.365 & 0.328 & 0.306 \\ C_2 & 0.297 & 0.335 & 0.368 \\ C_3 & 0.345 & 0.336 & 0.319 \\ C_4 & 0.416 & 0.332 & 0.252 \end{bmatrix}. \quad (15)$$

It can be seen from the weight table of the indicators that the entropy weight results obtained by only changing the basalt fiber content are similar to the entropy weight results obtained by only changing the diameter and length of basalt fibers, but the contribution rate is different. The water permeability coefficient has the greatest impact on the overall benefit evaluation of pervious concrete performance. At this time, the water permeability coefficient contributes 74.35% to the total efficiency. In the evaluation of total efficiency, the splitting tensile strength still occupies the second place, with a contribution rate of 13.77%, but there is still a big difference between the contribution rate and the permeability coefficient which has the greatest influence on the efficiency. The second is the compressive strength, and its contribution rate is not much different from that of the splitting tensile strength, accounting for 9.85%. The contribution of porosity in the evaluation is still the smallest, and the weight is also the smallest, accounting for only 2.04%. Finally, the product of the j-th evaluation index of the i-th sample in the standardized matrix and the j-th index weight w_j is used as the evaluation index F_i, and the calculation results of the evaluation index for different basalt fiber contents in Table 12 are obtained by calculating according to formula (10).

$$F_i^k = \sum w_j^k \times X_{ij}^k F_i^k = \begin{bmatrix} C_1 & C_2 & C_3 & C_4 \\ 0.099 & 0.138 & 0.020 & 0.743 \end{bmatrix} \times \begin{bmatrix} M_1 & M_2 & M_3 \\ 0.365 & 0.328 & 0.306 \\ 0.297 & 0.335 & 0.368 \\ 0.345 & 0.336 & 0.319 \\ 0.416 & 0.332 & 0.252 \end{bmatrix} = \begin{bmatrix} M_1 & M_2 & M_3 \\ 0.393 & 0.332 & 0.275 \end{bmatrix}. \quad (16)$$

From the calculation results of the evaluation index in Table 12, it can be seen that the selection of basalt fiber with a dosage of 2 kg/m^3 makes the utility value of each performance index reach the optimum, and the evaluation index is 0.393 at this time. Therefore, 2 kg/m^3 is selected as the optimal incorporation index of basalt fiber content.

5. Conclusion

In order to solve the problem that the permeability coefficient and strength of pervious concrete pavement are difficult to coordinate, the optimal incorporation index of basalt fiber to improve the strength of pervious concrete is obtained on the premise of ensuring the permeability of pervious concrete. In this paper, the basalt fiber was

incorporated into pervious concrete, and the single factor control variable method was used to carry out the test of basalt fiber modified pervious concrete, combined with the microstructure image basalt fiber is studied in different diameters, lengths, and dosages of permeable concrete mechanics performance, the influence law of permeable performance, and through the entropy method, the incorporation indexes of different basalt fibers were comprehensively compared and analyzed, and the following conclusions are drawn:

(1) Incorporating an appropriate amount of basalt fiber can enhance the mechanical properties of pervious concrete on the premise of satisfying the water permeability. Among them, when the diameter of basalt fiber increases from 14 μm to 20 μm, the compressive strength of pervious concrete decreases by 17.79%. The splitting tensile strength first increased and then decreased. Both porosity and permeability showed an increasing trend, increasing by 2.55% and 48.66%, respectively.

(2) When the length of basalt fiber increases from 12 mm to 24 mm, the compressive strength of pervious concrete increases continuously, with a relative increase of 20.54%. The splitting tensile strength first increased and then decreased. The permeability coefficient and porosity increased by 6.40% and 57.68%, respectively.

(3) With the increase of basalt fiber content, when the basalt fiber content increases from 2 kg/m^3 to 6 kg/m^3, the compressive strength of pervious concrete decreases by 16.25%. The splitting tensile strength was increased by 23.72%. The porosity and permeability decreased by 7.75% and 39.36%, respectively.

(4) This paper calculates the weight of each performance index bases on the experimentally measured data and adopted entropy theory, and finally obtains the results that conform to the objective result. It shows that the optimum incorporation index of basalt fiber in pervious concrete is 20 μm in diameter, 24 mm in length, and 2 kg/m^3 in content.

To sum up, this paper puts forward the technical idea of preparing ecologically permeable concrete by mixing basalt fiber and obtains the optimal mixing index of basalt fiber through a comprehensive analysis of the entropy method, which better solves the key problem that the permeability coefficient and strength of permeable concrete are difficult to coordinate, and hopes to provide a reference value for further research on basalt fiber permeable concrete.

Data Availability

The data used to support the findings of this study are included in this published article.

Conflicts of Interest

The authors declare that they have no conflicts of interest.

Acknowledgments

This research was funded by the Science and Technology Development Project of Jilin Province "Research on Key Technology of Application of Basalt Fiber Permeable Concrete in Permeable Pavement of Sponge City in Seasonal Frozen Area" (grant numbers 20210203143SF). This research was also funded by the Jilin Province Science and Technology Development Project "Study on performance and mechanism of inorganic binder for carbonated soil pavement reinforcement" (grant numbers YDZJ202201ZYTS647).

References

[1] W. H. Sun, *Experimental Research and Mix Proportion Design of Porous Concrete Based on Ort-Hogonal Test Method*, Southwest Jiao Tong University, Chengdu, China, 2016.

[2] C. Y. Lu, "Review on performance and application of pervious concrete," *Jushe*, vol. 3, p. 187, 2020.

[3] P. Shen, J. X. Lu, and H. Zheng, "Conceptual design and performance evaluation of high strength pervious concrete," *Construction and Building Materials*, vol. 269, Article ID 121342, 2021.

[4] W. Z. Wang, *Experimental Study on the Road Performance of Basalt Fiber Permeable Concrete*, Changchun Institute of Technology, Chengdu, China, 2020.

[5] W. T. Xue, *Experiment Study on Properties of Basalt Fiber Pervious Concrete*, Shanghai Jiao Tong University, Shangai, China, 2018.

[6] W. Q. Fang, W. Y. Dong, W. T. Xue, and J. C. Yang, "Study on properties of basalt fiber reinforced pervious concrete," *Concrete*, vol. 10, pp. 94–97, 2020.

[7] R. Z. Xu, M. M. Gui, and M. Z. Gong, "Study on the influence of different forming methods on the properties of pervious concrete," *Concrete*, vol. 11, pp. 129–131, 2011.

[8] D. M. Jiang, H. L. Cheng, and Z. L. Gao, "Development of pervious concrete pavement brick," *New Building Materials*, vol. 3, pp. 18–20, 2003.

[9] A. Radlińska, A. Welker, K. Greising, B. Campbell, and D. Littlewood, "Long-term field performance of pervious concrete pavement," *Advances in Civil Engineering*, vol. 2012, Article ID 380795, 9 pages, 2012.

[10] R. Q. Xie, *Experimental Study on Recycled Aggregate Pervious Concrete Base Material of Construction Waste*, Guangzhou University, Guangzhou, China, 2018.

[11] X. C. Zhang, *Study on Mix Design and Life Cycle Environmental Assessment System of High Performance Pervious Concrete*, Central South University, Changsha, China, 2012.

[12] C. P. Liu, *Experimental Study on Shrinkage Performance of Pervious Concrete*, North China University of Technology, Beijing, China, 2009.

[13] D. H. Nguyen and N. Sebaibi, "A modified method for the design of pervious concrete mix," *Construction and Building Materials*, vol. 73, pp. 271–282, 2014.

[14] J. Yang and G. Jiang, "Experimental study on properties of pervious concrete pavement materials," *Cement and Concrete Research*, vol. 33, pp. 381–386, 2003.

[15] K. X. Wu, L. B. Qian, and J. Y. Tan, "Development and engineering application of pervious concrete for sponge city," *New Building Materials*, vol. 11, pp. 119–122, 2018.

[16] D. F. Xu, "Study on the influence of porosity and size effect on mechanical properties of pervious concrete," *Commercial Concrete*, vol. 5, pp. 44–46, 2017.

[17] L. Guo, S. Y. Liu, and S. K. Chen, "Study on mechanical properties, water permeability and wear resistance of fiber modified recycled aggregate pervious concrete," *Transactions of the Chinese Society of Agricultural Engineering*, vol. 1, pp. 153–160, 2019.

[18] S. D Ahmed, Al Ridha, A. A. Abbood, and A. F. Atshan, "Assessment of the effect of replacing normal aggregate by porcelinite on the behaviour of layered steel fibrous self-compacting reinforced concrete slabs under uniform load," *Journal of Engineering*, vol. 2020, Article ID 3650363, 13 pages, 2020.

[19] N. Wang, K. F. Zhang, and S. R. Zhao, "Study on mechanical properties and water permeability of steel slag pervious concrete," *Commercial Concrete*, vol. 2, pp. 51–53, 2016.

[20] Z. G. Yin, K. Zhang, and Y. Zhao, "Frost durability test of recycled aggregate pervious concrete based on pore structure characteristics," *Bulletin of the Chinese Ceramic Society*, vol. 39, no. 3, pp. 756–761+778, 2020.

[21] W. Qiao, H. Zhang, F. Zhu, and Q. Wu, "A crack identification method for concrete structures using improved U-net convolutional neural networks," *Mathematical Problems in Engineering*, vol. 2021, Article ID 6654996, 16 pages, 2021.

[22] L. Zhao, T. Yan, X. Bai, T. Li, and J. Cheng, "Implementation of fictitious crack model using contact finite element method for the crack propagation in concrete under cyclic load," *Mathematical Problems in Engineering*, vol. 2013, Article ID 726317, 8 pages, 2013.

[23] J. Xie, J. Li, Z. Lu, and H. Zhang, "Experimental study on fatigue behaviour of BFRP-concrete bond interfaces under bending load," *Shock and Vibration*, vol. 2018, Article ID 7497061, 11 pages, 2018.

[24] S. Nagajothi, S. Elavenil, S. Angalaeswari, L. Natrayan, and P. Paramasivam, "Cracking behaviour of alkali-activated aluminosilicate beams reinforced with glass and basalt fibre-reinforced polymer bars under cyclic load," *International Journal of Polymer Science*, vol. 2022, Article ID 6762449, 13 pages, 2022.

[25] H. Dilbas and H. Çakir, "Influence of basalt fiber on physical and mechanical properties of treated recycled aggregate concrete," *Construction and Building Materials*, vol. 254, Article ID 119216.

[26] A. Sadrmomtazi, B. Tahmouresi, and A. Saradar, "Effects of silica fume on mechanical strength and microstructure of basalt fiber reinforced cementitious composites (BFRCC)," *Construction and Building Materials*, vol. 162, pp. 321–333, 2018.

[27] N. Rathod, M. Gonbare, and M. Pujari, "Basalt fiber reinforced concrete," *International Journal of Science and Research (IJSR) ISSN (Online Index Copernicus Value Impact Factor*, vol. 14, no. 5, pp. 2319–7064, 2013.

[28] C. Huang, *Study on Properties of Water Purification Basalt Fiber Permeable Cement Concrete*, South China University of Technology, Guangzhou, China, 2020.

[29] J. F. Huang, F. S. Wang, and H. Cui, "Effect of preparation technology on dispersion of polyvinyl alcohol fiber in recycled aggregate pervious concrete," *Silicate Bulletin*, vol. 38, no. 3, pp. 896–900, 2019.

[30] Y. X. Zhang, *Study on Properties of Basalt-polypropylene Hybrid Fiber Pervious Concrete*, Jiangxi University of Science and Technology, Jiangxi, China, 2021.

[31] Chinese standard, "Standard for test methods of concrete physical and mechanical properties (GB/T 50081-2019)," Chinese standard, Republic of China, 2019.

[32] "Technical specification for pervious concrete pavement (draft for Comments on partial revision Provisions)".

[33] "Technical specification for permeable cement concrete pavement (CJJ/T 135-2009)," 2009.

[34] J. X. Liu, *Experimental Study on Properties of Multi-Size Basalt Fiber Permeable Concrete*, North China University of Science and Technology, Qinhuangdao, China, 2019.

[35] M. M. Wang, *Development and Performance Test of Basalt Fiber Permeable Concrete*, Zhongyuan University Of Technology, Zhongyuan, China, 2020.

[36] S. Paulraj, N. Balasundaram, and K. Sates Kumar, "Experimental studies on strength and SCC characteristics of basalt fiber reinforced concrete," *International Journal of Civil Engineering*, vol. 8, pp. 704–711, 2017.

[37] Y. Wang, S. Zhang, and D. Niu, "Strength and chloride ion distribution brought by aggregate of basalt fiber reinforced coral aggregate concrete," *Construction and Building Materials*, vol. 234, Article ID 117390, 2020.

[38] D. Niu, L. Su, and Y. Luo, "Experimental study on mechanical properties and durability of basalt fiber reinforced coral aggregate concrete," *Construction and Building Materials*, vol. 237, Article ID 117628, 2020.

[39] Y. L. Lu, Z. G. Chen, and Z. G. Liu, "Study on agricultural water use efficiency in hebei Province based on entropy method," *Agricultural Resources And Regionalization in China*, vol. 36, no. 3, pp. 136–142, 2015.

[40] X. G. Guo, "Entropy method and its application in comprehensive evaluation," *Finance Research*, no. 6, pp. 56–60, 1994.

[41] F. X. Wang, A. H. Mao, H. L. Li, and M. L. Jia, "Quality measurement and spatial difference analysis of urbanization in shandong Province based on entropy method," *Geographical Science*, vol. 33, no. 11, pp. 1323–1329, 2013.

[42] F. F. Xu, *Research on Evaluation of Regional Innovation Capability Based on Entropy Method in China*, Shenyang University of Technology, Shenyang, China, 2013.

[43] J. Hao and S. J. Zhang, "Evaluation of provincial ecological data in China based on entropy method," *Information Science*, vol. 39, no. 1, pp. 157–162, 2021.

[44] Y. T. Shen and H. F. Jin, "Research on early warning system of Chinese local government debt risk -- based on analytic Hierarchy process and entropy method," *Modern finance and economics*, no. 6, pp. 34–46, 2019.

[45] Y. S. Cai and J. W. Lu, "Research on quality evaluation of beijing-tianjin-hebei regional development based on entropy method," *Industrial Technical Economy*, vol. 37, no. 11, pp. 67–74, 2018.

[46] X. Y. Tian, "Measurement of urbanization level in China based on entropy method," *Reforma*, vol. 5, pp. 151–159, 2018.

[47] H. Wang and Y. C. Guo, "Influence of linear dimensionless method on index weight of entropy M-ethod," *Population Resources and Environment in China*, vol. 27, no. S2, pp. 95–98, 2017.

[48] W. Wang, D. N. Liu, and D. Peng, "Safety extension evaluation of deep foundation pit excavation in sandy cobble stratum based on entropy method," *Journal of Southwest Jiaotong University*, vol. 56, no. 4, pp. 785–791+838, 2021.